



## Mangosteen Peel Extract (*Garcinia mangostana* L.) as a Potential Complementary of Leukemia Therapy: In Vitro and In Silico Studies

Marisca Evalina Gondokesumo<sup>1,\*</sup>, Arina Novilla<sup>2</sup>, Sijani Prahastuti<sup>3</sup>, Fadhilah Haifa Zahiroh<sup>4</sup>, Hanna Sari Widya Kusuma<sup>4</sup>, Wahyu Widowati<sup>3</sup>, Rizal Azis<sup>4,5</sup>, Dhanar Septyawan Hadiprasetyo<sup>4,6</sup>, Aris Muhammad Nurjamil<sup>4</sup>, Wahyu Surakusumah<sup>7</sup> & Khoerotul Nur Fadhilah Adha<sup>8</sup>

<sup>1</sup>Faculty of Pharmacy, University of Surabaya, Universitas Surabaya, Surabaya 60284, Indonesia

<sup>2</sup>Medical Laboratory Technology Study Program, Universitas Jenderal Achmad Yani, Cimahi 40531, Indonesia

<sup>3</sup>Faculty of Medicine, Maranatha Christian University, Bandung 40164, Indonesia

<sup>4</sup>Biomolecular and Biomedical Research Center, Aretha Medika Utama, Bandung 40163, Indonesia

<sup>5</sup>Biomedical Engineering, Department of Electrical Engineering, Faculty of Engineering, Universitas Indonesia, Depok 16424, Indonesia

<sup>6</sup>Faculty of Pharmacy, Universitas Jenderal Achmad Yani, Cimahi 40531, Indonesia

<sup>7</sup>Biology Study Program, Faculty of Mathematics and Science Education, Universitas Pendidikan Indonesia, Bandung 40154, Indonesia

<sup>8</sup>Biology Study Program, Faculty of Mathematics and Science Education, Universitas Negeri Jakarta, Jakarta 13220, Indonesia

\*E-mail: mariscaevalina@gmail.com, marisca@staff.ubaya.ac.id

**Abstract.** Leukemia is caused by abnormal white blood cell proliferation that leads to disruption of conventional blood cell functions. Mangosteen (*Garcinia mangostana* L.) contains phytochemical compounds with strong anticancer properties, according to various cancer studies. This study investigated the potential of mangosteen peel extract (MPE) as an anti-leukemia agent through molecular docking of LC-MS-identified compounds against FLT-1 and AKT proteins, followed by in vitro evaluation on HL-60 cells, namely cytotoxic (WST-8 assay), ROS levels and senescence (flow cytometry), and then *FLT1* and *AKT* gene expression (qRT-PCR). LC-MS identified  $\alpha$ -mangostin,  $\beta$ -mangostin,  $\gamma$ -mangostin, mangostinone, and epicatechin as the main compounds. Molecular docking revealed strong binding affinities from  $-8.5$  to  $-9.9$  kcal/mol against AKT, and from  $-9.0$  to  $-9.9$  kcal/mol against FLT-1. MPE (500  $\mu\text{g/mL}$ ) decreased cell viability and increased inhibition of HL-60 cells. Intracellular ROS levels decreased significantly at 0.6, 1.2, and 2.4  $\mu\text{g/mL}$  MPE. MPE induced cell senescence especially at 1.2 and 2.4  $\mu\text{g/mL}$ . Gene expression

---

Received September 4<sup>th</sup>, 2024, Revised July 20<sup>th</sup>, 2025, Accepted for publication December 30<sup>th</sup>, 2025  
 Copyright © 2025 Published by ITB Institut for Research and Community Service, ISSN: 2337-5760,  
 DOI: 10.5614/j.math.fund.sci.2025.57.2.3

analysis revealed downregulation of *AKT* at 1.2 and 2.4  $\mu\text{g/mL}$  and *FLT1* at 2.4  $\mu\text{g/mL}$ . These findings suggest that MPE may exert multifactorial anti-leukemic mechanisms, including apoptosis, ROS modulation, senescence induction, and regulation of *AKT* and *FLT1* expression.

**Keywords:** anticancer; cytotoxicity; *Garcinia mangostana*; HL-60 cell; leukemia.

## 1 Introduction

Leukemia is a group of hematological malignancies characterized by the abnormal proliferation of immature white blood cells [1]. Globally, leukemia ranked fifteenth in cancer incidence and eleventh in cancer-related mortality in 2020, highlighting its significant health burden [2]. Although its exact etiology remains unclear, leukemia is believed to arise from a complex interplay of genetic predisposition and environmental factors [3]. Isotretinoin has been reported as an alternative treatment in cases of poorly differentiated leukemia when conventional chemotherapy is contraindicated, resulting in complete hematological remission [4]. However, isotretinoin therapy is associated with notable hematological adverse effects and severe teratogenic risks, limiting its clinical application [5,6].

In recent years, herbal medicines have gained attention as potential complementary therapies for leukemia. Mangosteen peel extract (MPE) exhibits antioxidant, anti-inflammatory, and antiproliferative activities against cancer cells [7]. *Garcinia* species are rich in xanthenes, including  $\alpha$ -mangostin,  $\beta$ -mangostin,  $\gamma$ -mangostin, mangostinone A and B, and mangostenol, which contribute to their biological activity [8]. Xanthenes have demonstrated synergistic apoptotic effects when combined with chemotherapeutic agents such as bortezomib in leukemia cells [9], as well as inhibitory activity against receptor tyrosine kinases such as EGFR and VEGFR2, suggesting their potential as targeted anti-leukemic agents [10-12]. Despite these findings, most studies have focused on isolated biological effects or single molecular targets. Therefore, a more integrated evaluation of MPE is warranted.

The phosphoinositide 3-kinase/protein kinase B (PI3K/AKT) signaling pathway plays a critical role in normal and malignant hematopoiesis and represents an important therapeutic target in leukemia. Dysregulation of this pathway promotes leukemic cell survival, proliferation, and drug resistance, while FLT-1-mediated signaling supports angiogenesis and leukemia progression through microenvironmental interactions [13]. PI3K/AKT signaling involves the mTORC1 and mTORC2 complexes, which regulate cell growth, apoptosis, and autophagy. FLT-1, is primarily known for its role in angiogenesis and has

been increasingly implicated in cancer progression, further supporting its relevance in leukemia research [14].

Evaluation of the cytotoxic effects of herbal extracts is essential for understanding their influence on leukemia cell viability, oxidative stress, and tumor microenvironments [15]. Modulation of reactive oxygen species (ROS), cell cycle progression, senescence, and apoptosis represents key mechanisms underlying their anticancer potential [16]. Accordingly, this study investigated the anti-leukemic potential of MPE through molecular docking of LC-MS-identified compounds against FLT-1 and AKT proteins, followed by *in vitro* evaluation on HL-60 cells, including cytotoxicity, ROS levels, senescence, and *AKT* and *FLT1* gene expression.

## 2 Materials and Methods

### 2.1 Preparation of Mangosteen Peel Extract (MPE) and LC-MS Assay

Extraction of MPE was conducted by the Borobudur Natural Herbal Industry (Semarang, Indonesia) following Good Manufacturing Practices (GMP) standards and was assigned to CoA No. Batch 111PV01.1. Mangosteen peels were extracted with 70% ethanol, followed by the addition of maltodextrin. Qualitative analysis and identification of bioactive components were performed using liquid chromatography-mass spectrometry (LC-MS) [17,18].

### 2.2 Biological Activity Prediction

The mangosteen compounds underwent additional analysis to determine their biological activities relevant to anticancer mechanisms. The isomeric SMILES of every molecule was entered into the WAY2DRUG PASS website to predict the biological activity; the Pa (probability of activity) value was displayed as a result. In this investigation, a cut-off score of 0.7 of Pa was employed for every biological activity [19].

### 2.3 ADMET Compounds Prediction

Absorption, Distribution, Metabolism, Excretion, and Toxicity (ADMET) analysis was performed to evaluate the pharmacokinetic and safety profiles of the compounds with anti-inflammatory potential. ADMET prediction was conducted using the Protox 3.0 platform [20]. Drug-likeness was assessed based on Lipinski's Rule of Five, which predicts metabolic feasibility by comparing compounds with known drugs. According to these criteria, acceptable compounds generally exhibit a molecular weight < 500 Da, LogP < 5, fewer than five hydrogen bond donors, and fewer than ten hydrogen bond acceptors.

Toxicity classification was determined using predicted LD<sub>50</sub> values, ranging from Class I (extremely toxic, LD<sub>50</sub> ≤ 5 mg/kg) to Class VI (least toxic, LD<sub>50</sub> > 5000 mg/kg) [19].

## 2.4 Molecular Docking

The anti-inflammatory potential of mangosteen was evaluated by molecular docking targeting FLT-1 and AKT proteins. Protein structures (PDB IDs: 3HNG and 3O96) were obtained from the RCSB database and validated by redocking of native ligands with RMSD ≤ 2 Å. Ligands retrieved from PubChem were energy-minimized using UCSF Chimera, prepared with AutoDock 4.2, and docked using AutoDock Vina. Binding affinities were calculated, and protein-ligand interactions were visualized using Discovery Studio.

## 2.5 HL-60 Cell Cultivation

Human acute promyelocytic cells (HL-60) were procured from Aretha Medika Utama, Indonesia. The cell lines were cultivated in a culture medium that contained Iscove's Modified Dulbecco's Medium (IMDM) from Gibco (12440-053) supplemented with Biowest reagents, including 10% fetal bovine serum (FBS) (S181B-500), 1% L-glutamine (X0550-100), 1% amphotericin B (L0009-050), 1% minimum essential medium vitamins (X0556-100), 1% nanomycopolitine (L-X16-100), 1% antibiotic-antimycotic (L0010-100), and 0.1% gentamicin (Gibco, 15750060). The cells were incubated in a humidified incubator (Thermo IH3543) maintained at 37 °C with 5% CO<sub>2</sub> to support optimal cell growth. After 24 h, cell viability was evaluated using a Neubauer hemocytometer with trypan blue exclusion staining (Gibco, 15250-100), ensuring an adequate number of viable cells for subsequent cytotoxicity testing and additional experimental procedures [18].

## 2.6 Cytotoxic Assay

In 96-well plates (Costar, 3596),  $1 \times 10^4$  cells were seeded per well and grown at 37 °C with 5% CO<sub>2</sub>. 90 µL of medium culture and 10 µL of MPE at different concentrations (3.7, 7.8, 15.6, 31.5, 62.5, 125, 250, and 500 µg/mL) was added in place of the culture medium. For 24 h, the cells were incubated. After that, 10 µL of CCK-8 buffer (Elabscience, E-CK-A362) was added to each well, which was then incubated for 3 h. A spectrophotometer (Multiskan GO Thermo Scientific 51119300) was used to measure the absorbance at 450 nm [18]. The proportion of live cells, cell inhibition, and median inhibitory concentration (IC<sub>50</sub>) were the metrics used to express the results. The experimental treatments were carried out using IC<sub>50</sub> values of 0.6, 1.2, and 2.4 µg/mL.

## 2.7 Reactive Oxygen Species Assay

Flow cytometry (MAQS Quant, Analyzer 10, Miltenyi Biotec), employing a ROS Fluorometric Assay Kit from Elabscience (E-BC-K138-F) was utilized to detect intracellular ROS levels. Five different groups were established: (NC) negative control; (DMSO) vehicle control prepared from 10% DMSO stock solution, further diluted in culture medium to a final concentration of  $\leq 0.5\%$ ; (MPE 0.6) MPE 0.6  $\mu\text{g}/\text{mL}$ ; (MPE 1.2) MPE 1.2  $\mu\text{g}/\text{mL}$ ; and (MPE 2.4) MPE 2.4  $\mu\text{g}/\text{mL}$ . After treatment, the medium was removed and 1 mL of DCFH-DA (10  $\mu\text{M}$ ) was added. The cells were incubated at 37 °C for 60 mins and ROS levels were then measured using a flow cytometer. The fluorescence levels obtained were represented as percentages compared to the control group [21].

## 2.8 Senescence Assay

The Senescence Cells Histochemical Staining Kit from Sigma (CS0030) was used to study senescence cells. After cultivating the cells on 6-well plates, these were exposed to MPE 0.6, 1.2, and 2.4  $\mu\text{g}/\text{mL}$  for 24 h. PBS 1x was used to rinse the cells. Before being rinsed once more with PBS 1x, the cells were fixed for 7 mins in 1x fixation buffer. Each well was filled with the staining mixture and the cells were maintained overnight at 37 °C without CO<sub>2</sub>. Under a light microscope, the cell staining results were obvious [21].

## 2.9 Real-time PCR (RT-PCR)

Direct-zol RNA Miniprep Plus (Zymo Research, R2073) and TRI Reagent (Zymo Research, R2050-1-200) were utilized as per the instructions of the manufacturer to isolate total RNA from HL-60 cells. RNA concentration was determined using a spectrophotometer at 260 and 280 nm. The purity and concentration of RNA are shown in Table 1.

**Table 1** Concentration and RNA purity for Real-Time PCR.

Sample	Concentration (ng/ $\mu\text{L}$ )	Purity ( $\lambda 260/\lambda 280$ nm)
NC	7.2	2.185
DMSO	2.72	1.595
MPE 0.6 $\mu\text{g}/\text{mL}$	8.72	2.551
MPE 1.2 $\mu\text{g}/\text{mL}$	1.6	1.807
MPE 2.4 $\mu\text{g}/\text{mL}$	10.8	1.421

The complementary DNA (cDNA) was synthesized using the SensiFAST cDNA Synthesis Kit (Bioline, BIO-65054), with incubation steps of 25 °C for 5 mins, 46 °C for 20 mins, and 95 °C for 1 mins [22]. PCR amplification was

conducted using the AriaMx Real-Time PCR System from Agilent (G8830A). The qPCR program began with pre-denaturation at 95 °C for 5 mins, followed by 40 cycles of denaturation at 95 °C for 50 secs, annealing at 58 °C for *GAPDH* and 60 °C for *FLT1* and *AKT* for 50 secs, and elongation at 72 °C for 50 secs. *GAPDH* served as the housekeeping gene, and the primer sequences are provided in Table 2.

**Table 2** Primers for qRT-PCR.

Gene	Primer Sequences (5' - 3')		References
	Forward	Reverse	
<i>GAPDH</i> (Human)	GCCAAAAGGGTCATC ATCTC	TGAGTCCTTCCACGATAC CA	NM_001357943.2
<i>AKT</i> (Human)	ACCTCAAGCTGGAGA ACCT	ATCTCGTACATGACCACG C	NM_001382431.1
<i>FLT1</i> (Human)	CTGGGCAGCAGACAA ATCCT	TGGAAGAGAAGCTTGTA GGTGG	NM_001160031.1

## 2.10 Statistical Analysis

All assays were conducted as three independent replicates. The  $IC_{50}$  values were determined by probit regression analysis using the SPSS Statistics software (version 20.0; IBM, USA). Data are expressed as the mean  $\pm$  standard deviation (SD). Differences among experimental groups were evaluated using one-way ANOVA, followed by Tukey's multiple comparison test. Statistical significance was defined at  $p < 0.05$ .

## 3 Results

### 3.1 Compound Analysis in Mangosteen Peel Extract (MPE) by LC-MS

The various compounds were characterized based on their molecular weights as determined by chromatogram peaks (Figure 1). The outcomes of our LC-MS analysis were compared against a set of standard compounds with the following molecular weights:  $\alpha$ -mangostin (410.5 g/mol),  $\beta$ -mangostin (424.5 g/mol),  $\gamma$ -mangostin (396.4 g/mol), gartanin (396.4 g/mol), mangostinone (380.4 g/mol), garcinone D (428.5 g/mol), and epicatechin (290.27 g/mol).

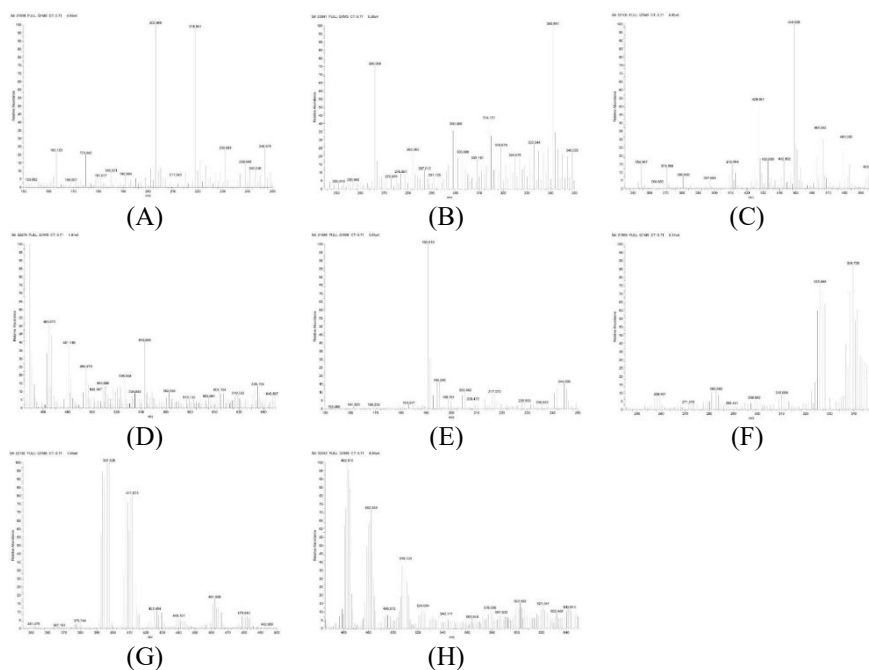


**Figure 1** LC-MS spectrum of MPE. (A) Mass spectra 150 to 250 m/z with positive ionization, (B) mass spectra 250 to 350 m/z with positive ionization, (C) mass spectra 350 to 500 m/z with positive ionization, (D) mass spectra 450 to 650 m/z with positive ionization, (E) mass spectra 150 to 250 m/z with negative ionization, (F) mass spectra 250 to 350 m/z with negative ionization, (G) mass spectra 350 to 500 m/z with negative ionization, and (H) mass spectra 450 to 650 m/z with negative ionization.

**Table 3** Identification of target compounds in MPE with LC-MS.

Compounds in MPE	MW (g/mol)	MS [M+H] +	[M+N H4] <sup>+</sup>	[M+N a] <sup>+</sup>	[M+K] <sup>+</sup>	[M-H] <sup>-</sup>	[M+N a-2H] <sup>-</sup>	[M+Cl] <sup>-</sup>	[M+K -2H] <sup>-</sup>
$\alpha$ -mangostin	410.17	411.18	428.21	433.16	449.14	409.17	431.15	445.14	447.12
$\beta$ -mangostin	424.19	411.18	442.22	447.18	463.15	423.18	445.16	459.16	461.14
$\gamma$ -mangostin	396.16	397.17	414.19	419.15	435.12	395.15	417.13	431.13	433.11
mangostinone	380.16	381.17	398.20	403.15	419.13	379.16	401.14	415.13	417.11
epicatechin	290.08	291.09	308.11	313.07	329.04	289.07	311.05	325.05	327.03

These analytical results unequivocally demonstrated the presence of specific constituents within MPE, namely: 1)  $\alpha$ -mangostin, 2)  $\beta$ -mangostin, 3)  $\gamma$ -mangostin, 4) mangostinone, and 5) epicatechin (Table 3).

### 3.2 Biological Activity Prediction

The examination of the chemicals found in the MPE, focusing on their potential as antioxidant and anticancer agents, are presented in Table 4. The isomeric SMILES for each molecule was processed using the WAY2DRUG PASS tool, yielding the Pa (probability of activity) values. A cut-off score of 0.7 was applied to determine significant activity.

**Table 4** Prediction of compound in MPE as antioxidant and anticancer agent.

Compounds	Bioactivity	Pa	Pi
$\alpha$ -mangostin	Apoptosis agonist	0.875	0.005
	Antineoplastic	0.831	0.008
	Chemopreventive	0.739	0.005
	Free radical scavenger	0.795	0.003
$\beta$ -mangostin	Apoptosis agonist	0.871	0.005
	Antineoplastic	0.822	0.009
	Chemopreventive	0.724	0.006
	Free radical scavenger	0.765	0.003
	Antioxidant	0.703	0.004
$\gamma$ -mangostin	Apoptosis agonist	0.898	0.004
	Antineoplastic	0.834	0.008
	Chemopreventive	0.741	0.005
	Free radical scavenger	0.773	0.003
	Antioxidant	0.826	0.003
	Anticarcinogenic	0.734	0.007
mangostinone	Apoptosis agonist	0.866	0.005
	Antineoplastic	0.778	0.015
	Chemopreventive	0.829	0.003
	Free radical scavenger	0.882	0.002
	Antioxidant	0.772	0.004
	Anticarcinogenic	0.810	0.005
epicatechin	Chemopreventive	0.788	0.004
	Free radical scavenger	0.842	0.002
	Antioxidant	0.810	0.003
	Anticarcinogenic	0.795	0.005

### 3.3 ADMET Compounds Prediction on MPE as Antioxidant and Anticancer

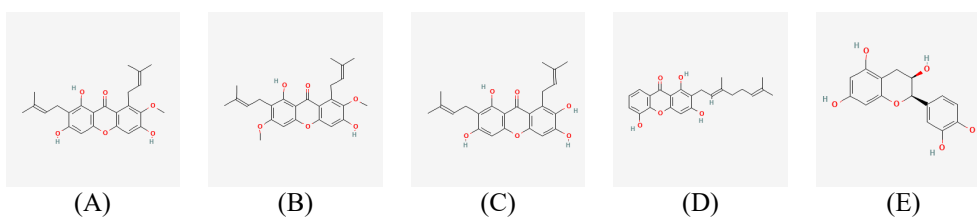
The characteristics of ADMET contribute to the discovery of new drugs (Table 5). The toxicity and LD<sub>50</sub> of these compounds show high values and are considered relatively low toxicity profiles. Both compounds did not have the potential to induce hepatotoxicity, neurotoxicity, carcinogenicity, or cytotoxicity. Hence, the compounds were used in further tests.

**Table 5** ADMET characteristics of compounds in MPE (Protox 3.0 prediction).

	$\alpha$ -mangostin	$\beta$ -mangostin	$\gamma$ -mangostin	mangostinone	epicatechin
LD <sub>50</sub> (mg/kg)	1500	1500	3200	1190	10000
Toxicity class	4	4	5	4	6
Average similarity (%)	54.5	55.58	53.58	100	100
Prediction accuracy (%)	67.38	67.38	67.38	100	100
Molecular weight	410.46	424.49	396.43	371.52	290.27
Number of H-bond acceptors	5	5	5	2	6
Number of H-bond donors	3	2	4	0	5
Number of atoms	30	31	29	28	21
Number of bonds	32	33	31	30	23
Number of rotatable bonds	5	6	4	8	1
Octanol/water partition coefficient (logP)	5.09	5.39	4.79	6	1.55

### 3.4 Molecular Docking

Compounds  $\alpha$ -mangostin,  $\beta$ -mangostin,  $\gamma$ -mangostin, mangostinone, and epicatechin were docked against FLT-1 and AKT proteins (Figure 2). Redocking confirmed the validity of the active sites, with RMSD values  $\leq 2$  Å. All compounds showed favorable interactions and occupied the active sites of both target proteins, indicating stable binding conformations (Figures 3 and 4). Interaction analysis revealed hydrogen bonding and hydrophobic interactions, while binding affinities varied among the compounds (Table 6). The strongest interactions were observed for  $\gamma$ -mangostin–AKT and mangostinone–AKT complexes, both exhibiting the lowest binding energy of 9.9 kcal/mol.



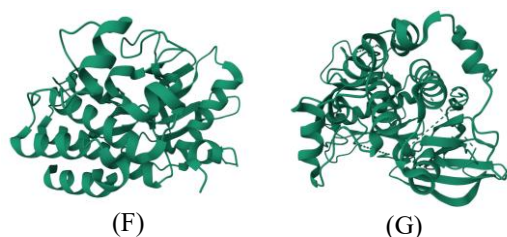


**Figure 2** 2D structures of selected compounds from MPE and the target proteins used in molecular docking. (A)  $\alpha$ -mangostin; (B)  $\beta$ -mangostin; (C)  $\gamma$ -mangostin; (D) mangostinone; (E) epicatechin; (F) FLT-1 (PDB ID: 3HNG); (G) AKT (PDB ID: 3O96).

**Table 6** Binding affinity values and amino acid residues from molecular interactions.

Compounds	FLT-1			AKT		
	Binding Affinity (kcal/mol)	Hydrogen Bond	Hydrophobic Interaction	Binding Affinity (kcal/mol)	Hydrogen Bond	Hydrophobic Interaction
$\alpha$ -mangostin	-9.4	ILE1019 ASP1040 ILE1038	ILE881 LEU882 VAL892 VAL909 CYS1039 VAL907	-9.7	ASN54 CYS296 VAL271	ILE84 ARG86 VAL270 TRP80
$\beta$ -mangostin	-8.5	ILE1019 GLU878	ILE881 VAL891 LEU1013 VAL892 VAL909 CYS1039 LEU882 VAL907	-9.8	ASN54 VAL271 CYS296	ILE84 ARG86 VAL270 TRP80
$\gamma$ -mangostin	-9.4	ARG1021 ILE1019 ASP1040 VAL892	ILE881 LEU882 LYS861 VAL907 VAL909 VAL892 CYS1039	-9.9	ASN54 CYS296	ILE84 ARG86 VAL270 LYS268 TRP80
mangostinone	-9.0	ILE1019	ALA859 VAL892 VAL909 LEU882 LYS861 VAL841 ILE881	-9.9	ASN54	TRP80 TYR272 VAL270 LEU264
epicatechin	-8.6	ASP1040 HIS1020 CYS1039	ILE881 LEU882	-9.0	ASN54 ASP292 THR211 ILE290 ASP292	VAL270 TRP80 THR291 ASP292 LEU210

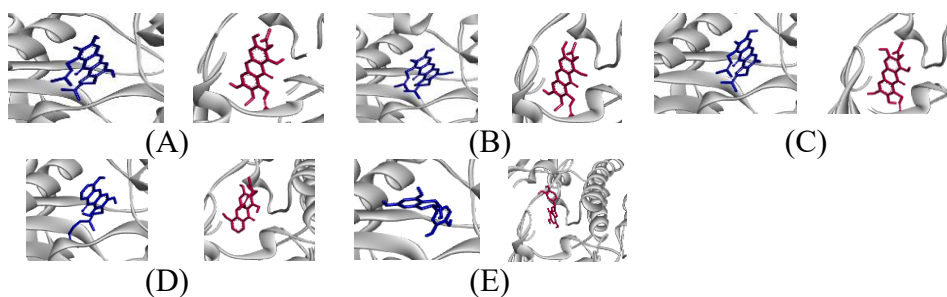


**Figure 3** 3D visualization of the molecular docking results. Blue compound represents the docking interaction with FLT-1 protein and red compound represents the docking interaction with AKT protein. (A)  $\alpha$ -mangostin; (B)  $\beta$ -mangostin; (C)  $\gamma$ -mangostin; (D) mangostinone; (E) epicatechin.

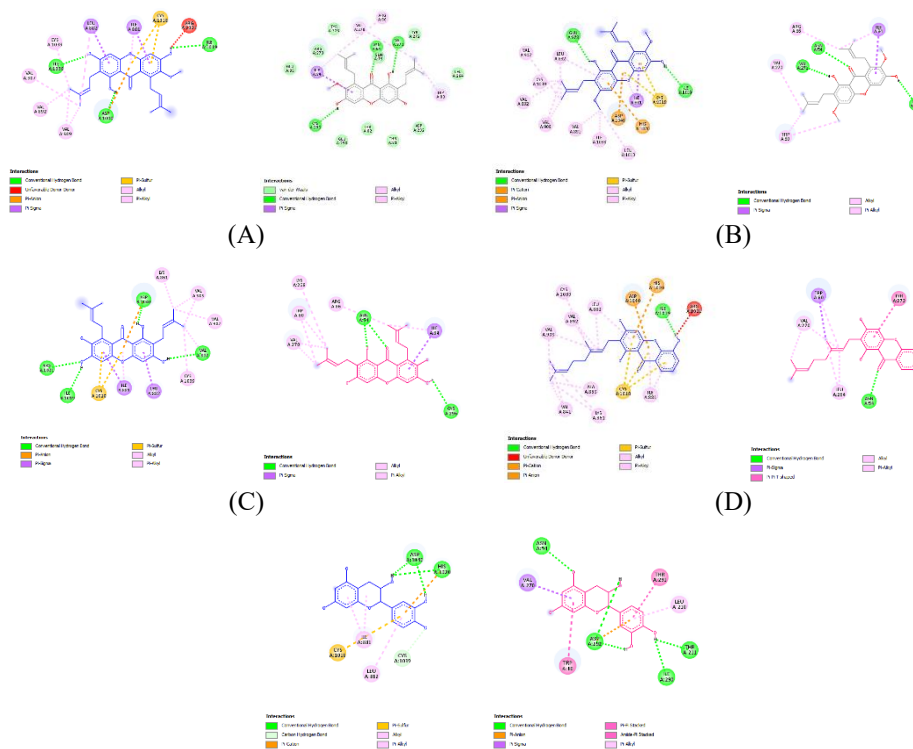


**Figure 4** 2D visualization of the molecular docking results. Blue compound represents the docking interaction with FLT-1 protein and red compound represents the docking interaction with AKT protein. (A)  $\alpha$ -mangostin; (B)  $\beta$ -mangostin; (C)  $\gamma$ -mangostin; (D) mangostinone; (E) epicatechin.

### 3.5 Cytotoxic Effect of MPE toward HL-60 Cells

Figure 5 illustrates the cytotoxic effect of MPE on HL-60 cells based on cell inhibition and viability. MPE exhibited the strongest cytotoxic activity at 500  $\mu\text{g}/\text{mL}$ , as indicated by a marked reduction in WST-8 absorbance compared to untreated controls. Inhibition values exceeding 100% reflected absorbance levels below the baseline, indicating severe cytotoxicity and complete loss of metabolic activity rather than true biological overestimation. This preliminary dose-screening assay was used to determine the  $\text{IC}_{50}$  value of MPE, which was calculated as 1.18  $\mu\text{g}/\text{mL}$ . Based on this value, concentrations of 0.6, 1.2, and 2.4  $\mu\text{g}/\text{mL}$  were selected for subsequent cellular and mechanistic analyses to ensure biologically relevant exposure while minimizing non-specific cytotoxic effects.

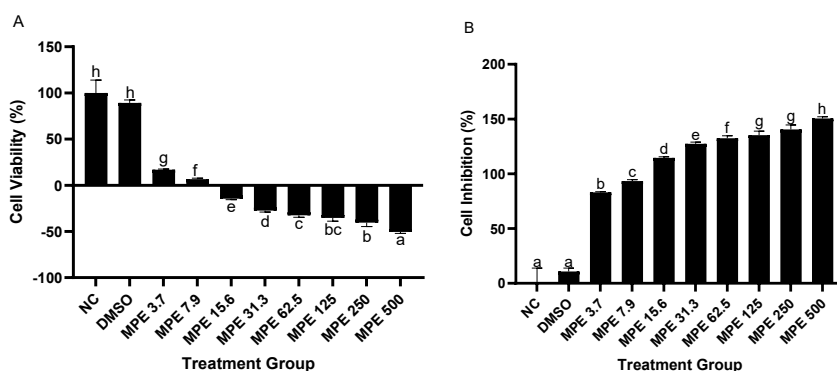


**Figure 5** The percentage cell viability (A) and cell inhibition (B) of HL-60 cells treated with MPE in eight different concentrations. NC: negative control, untreated HL-60 cells; DMSO: HL-60 cells with DMSO; MPE 3.7: HL-60 cells + MPE 3.7  $\mu\text{g}/\text{mL}$ ; MPE 7.9: HL-60 cells + MPE 7.9  $\mu\text{g}/\text{mL}$ ; MPE 15.6: HL-60 cells + MPE 15.6  $\mu\text{g}/\text{mL}$ ; MPE 31.3: HL-60 cells + MPE 31.3  $\mu\text{g}/\text{mL}$ ; MPE 62.5: HL-60 cells + MPE 62.5  $\mu\text{g}/\text{mL}$ ; MPE 125: HL-60 cells + MPE 125  $\mu\text{g}/\text{mL}$ ; MPE 250: HL-60 cells + MPE 250  $\mu\text{g}/\text{mL}$ ; MPE 500: HL-60 cells + MPE 500  $\mu\text{g}/\text{mL}$ . The independent-samples t-test showed a significant difference ( $p < 0.05$ ) between concentrations indicated by different letters in each bar.

### 3.6 Effect of MPE toward Reactive Oxygen Species Level

Figure 6 shows that MPE significantly reduced intracellular ROS levels in the HL-60 cells. The negative control exhibited the highest ROS production, while treatment with MPE at 0.6, 1.2, and 2.4  $\mu\text{g}/\text{mL}$  markedly decreased ROS levels compared to both the negative control and DMSO-treated cells. A

concentration-dependent reduction in ROS accumulation was observed, indicating the antioxidant and ROS-scavenging activity of MPE.

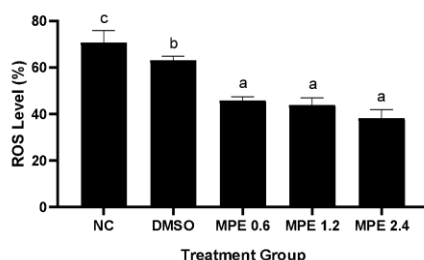


**Figure 6** Effect of MPE towards ROS level percentage in HL-60 cells. NC: negative control, untreated HL-60 cells; DMSO: HL-60 cells with DMSO; MPE 0.6: HL-60 cells + MPE 0.6  $\mu\text{g}/\text{mL}$ ; MPE 1.2: HL-60 cells + MPE 1.2  $\mu\text{g}/\text{mL}$ ; MPE 2.4: HL-60 cells + MPE 2.4  $\mu\text{g}/\text{mL}$ . Different letters represent a significant difference at  $p < 0.05$  (Tukey HSD) between concentrations.

### 3.7 Senescence Cells Percentage

Figure 7 shows that MPE induced cellular senescence in HL-60 cells. The negative control and DMSO groups did not exhibit significant senescence, whereas MPE treatment markedly increased the proportion of senescent cells. Higher MPE concentrations (1.2 and 2.4  $\mu\text{g}/\text{mL}$ ) produced greater senescence levels compared to 0.6  $\mu\text{g}/\text{mL}$ , indicating a dose-dependent senescence-inducing effect of MPE.

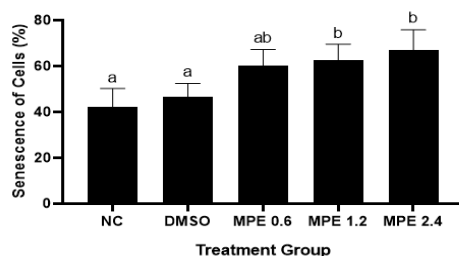


**Figure 7** Effect of MPE towards senescence cells percentage of the HL-60 cells. NC: negative control, untreated HL-60 cells; DMSO: HL-60 cells with DMSO; MPE 0.6: HL-60 cells + MPE 0.6  $\mu\text{g}/\text{mL}$ ; MPE 1.2: HL-60 cells + MPE 1.2  $\mu\text{g}/\text{mL}$ ; MPE 2.4: HL-60 cells + MPE 2.4  $\mu\text{g}/\text{mL}$ . Different letters represent a significant difference at  $p < 0.05$  (Tukey HSD) between concentrations.

### 3.8 *AKT* and *FLT1* Gene Expression Level

Figure 8A shows that *AKT* gene expression in the HL-60 cells remained unchanged in the negative control, DMSO group, and cells treated with 0.6  $\mu\text{g/mL}$  MPE. In contrast, MPE at 1.2 and 2.4  $\mu\text{g/mL}$  significantly reduced *AKT* mRNA expression, indicating a concentration-dependent inhibitory effect. As shown in Figure 8B, *FLT1* gene expression was not significantly affected by most treatments; however, MPE at 2.4  $\mu\text{g/mL}$  significantly decreased *FLT1* expression, suggesting that higher MPE concentrations are required to suppress *FLT1* gene expression.

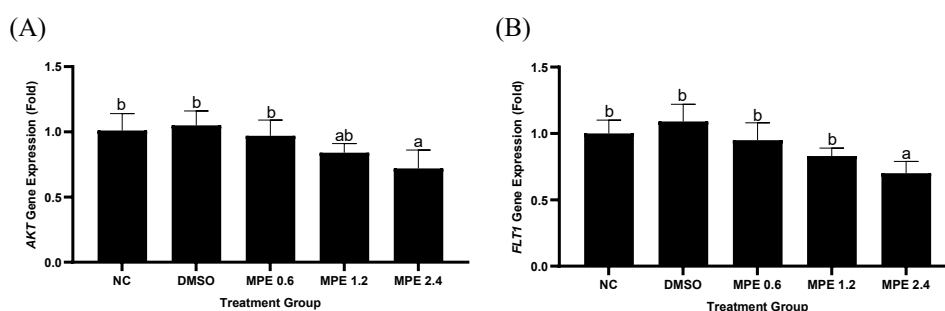


**Figure 8** Effect of MPE towards *AKT* (A) and *FLT1* (B) gene expression in HL-60 cells. NC: negative control, untreated HL-60 cells; DMSO: HL-60 cells with DMSO; MPE 0.6: HL-60 cells + MPE 0.6  $\mu\text{g/mL}$ ; MPE 1.2: HL-60 cells + MPE 1.2  $\mu\text{g/mL}$ ; MPE 2.4: HL-60 cells + MPE 2.4  $\mu\text{g/mL}$ . Different letters represent a significant difference at  $p < 0.05$  (Tukey HSD) between concentrations.

## 4 Discussion

$\alpha$ -Mangostin,  $\beta$ -mangostin, and epicatechin are well known for their anticancer activities [23], and mangosteen peel is a rich source of diverse xanthone compounds [24]. LC-MS analysis confirmed the presence of multiple xanthenes in mangosteen peel extract (MPE), including  $\alpha$ -mangostin,  $\gamma$ -mangostin, smeathxanthone, mangostenol, and garcimangosxanthone, highlighting the chemical diversity of MPE and supporting its biological potential. Xanthenes derived from various parts of mangosteen exhibit broad pharmacological activities, particularly anticancer effects mediated through apoptosis induction, protein interactions, and modulation of key signaling pathways [23,24].

Cytotoxicity assays serve as an essential preliminary screening to evaluate the effects of bioactive compounds on cancer cell viability and growth [25]. In this study, MPE exhibited strong cytotoxic activity against HL-60 leukemia cells, particularly at 500  $\mu\text{g/mL}$ , accompanied by reduced cell viability. These findings are consistent with previous reports showing that  $\alpha$ -mangostin and  $\beta$ -mangostin induce cytotoxic and pro-apoptotic effects across various cancer cell lines through mitochondrial dysfunction, caspase activation, and cell cycle arrest [26-29]. The degree of cytotoxicity observed aligns with established classifications of cell viability responses, where values below 40% indicate strong cytotoxic effects [30].

The PI3K/AKT signaling pathway plays a critical role in cancer cell survival, proliferation, and therapy resistance, particularly in leukemia and glioma [28]. Previous studies demonstrated that  $\beta$ -mangostin suppresses AKT phosphorylation and inhibits PI3K/AKT/mTOR signaling, thereby inducing apoptosis and reducing cancer cell proliferation [31]. In line with these findings, MPE in the present study significantly modulated *AKT* gene expression at higher concentrations, supporting its role in disrupting survival signaling pathways. Additionally, MPE induced cellular senescence and apoptosis in HL-60 cells, consistent with its antiproliferative and antitumor properties [33].

A notable finding was the dose-dependent modulation of intracellular ROS levels following MPE treatment. At lower concentrations, MPE acted as an antioxidant, reducing oxidative stress, while higher concentrations exhibited pro-oxidant effects that may contribute to ROS-mediated cytotoxicity and apoptosis. This biphasic behavior is characteristic of polyphenol-rich extracts and xanthone derivatives and is considered a key mechanism underlying their selective anticancer activity. Given the crucial role of oxidative stress in leukemia progression and treatment response, such dual activity may enhance the therapeutic relevance of MPE [40].

Gene expression analysis further revealed concentration-dependent regulation of *AKT* and *FLT1* following MPE exposure. Xanthenes have been reported to inhibit VEGF-FLT-1 signaling and downstream targets such as AKT and ERK1/2, thereby suppressing angiogenesis, cell migration, and survival pathways [34,35]. These findings are consistent with the observed molecular docking results, which demonstrated strong interactions between key xanthenes and AKT or FLT-1. Docking validation confirmed accurate binding sites with  $\text{RMSD} \leq 2 \text{ \AA}$  [41], and strong hydrogen bonding and hydrophobic interactions contributed to binding stability and affinity [42-44]. Compounds such as  $\alpha$ -mangostin,  $\gamma$ -mangostin, and mangostinone exhibited favorable binding

affinities toward AKT and FLT-1, providing mechanistic support for the in vitro cytotoxic effects observed.

In silico bioactivity prediction further supported the anticancer potential of MPE compounds, with  $P_a$  values  $> 0.7$  indicating strong predicted activities, including antineoplastic, apoptotic, antioxidant, and chemopreventive properties [38,39]. ADMET evaluation based on Lipinski's Rule of Five indicated that all tested compounds met key drug-likeness criteria, including acceptable molecular weight, hydrogen bond donors and acceptors, and lipophilicity. Notably, epicatechin and mangostinone demonstrated the most favorable ADMET profiles, suggesting good oral bioavailability potential [45-48].

Collectively, these findings support the potential of MPE as a complementary anti-leukemia agent. The integration of molecular docking, cytotoxicity assays, ROS modulation, and gene expression analysis indicates that xanthone-rich MPE may interfere with critical survival and resistance-related pathways, particularly AKT and FLT-1 signaling. Although the present study provides strong in vitro and mechanistic evidence, further investigations, including molecular dynamics simulations, in vivo leukemia models, and pharmacokinetic studies, are necessary to validate the efficacy, stability, and safety of MPE under physiologically relevant conditions.

## 5 Conclusion

MPE demonstrated therapeutic potential as a complementary agent for leukemia treatment. LC-MS analysis identified  $\alpha$ -mangostin,  $\beta$ -mangostin,  $\gamma$ -mangostin, mangostinone, and epicatechin as its main compounds. Molecular docking revealed strong binding affinities of these compounds to AKT and FLT-1 proteins. In vitro, MPE showed concentration-dependent cytotoxicity, reduced ROS levels, induced senescence in HL-60 cells, and downregulated *AKT* and *FLT1* gene expression. These findings collectively underscore the multifaceted therapeutic properties of MPE against HL-60 cells, suggesting its potential in leukemia treatment development and warranting further exploration. Importantly, these results support further investigation of standardized MPE fractions or isolated xanthenes in leukemia preclinical models to assess their translational and therapeutic relevance.

## Acknowledgements

The authors gratefully acknowledge the Competitive National Research–Fundamental Research 2023 program of the Ministry of Education, Culture, Research, and Technology of the Republic of Indonesia for financial support

under the Applied Research scheme (Grant No. 183/E5/PG.02.00.PL/2023). The authors also thank the Aretha Medika Utama Biomolecular and Biomedical Research Center for their valuable technical assistance and PT. Industri Jamu Borobudur prepared mangosteen peel extract.

## References

- [1] Hoseini, S.S., Espinosa-Cotton, M., Guo, H.F. & Cheung, N.K.V., *Overcoming Leukemia Heterogeneity by Combining T Cell Engaging Bispecific Antibodies*, Journal for Immunotherapy of Cancer, **8**(2), e001626, 2020.
- [2] Heidari-Foroosan, M., Saeedi Moghaddam, S., Keykhaei, M., Shobeiri, P., Azadnajafabad, S., Esfahani, Z. & Farzadfar, F., *Regional and National Burden of Leukemia and Its Attributable Burden to Risk Factors in 21 Countries and Territories of North Africa and Middle East, 1990–2019: Results From the GBD Study 2019*, Journal of Cancer Research and Clinical Oncology, **149**(8), pp. 4149-4161, 2023.
- [3] Du, M., Chen, W., Liu, K., Wang, L., Hu, Y., Mao, Y. & Ye, D., *The Global Burden of Leukemia and Its Attributable Factors in 204 Countries and Territories: Findings from The Global Burden of Disease 2019 Study and Projections to 2030*, Journal of Oncology, **2022**(1), 1612702, 2022.
- [4] Alkhalidy, H.Y., Assiri, A.M., Fatima, S. & Owaidah, T., *Isotretinoin Is Active in The Initial Management of Acute Pro-myelocytic Leukemia*, Leukemia Research Reports, **14**, 100220, 2020.
- [5] Demirci Saadet, E. & Sahin, U., *Evaluation of Hematological Parameters in Patients Using Systemic Isotretinoin with Diagnosis of Acne Vulgaris*, Journal of Cosmetic Dermatology, **22**(3), pp. 1077-1082, 2023.
- [6] Draghici, C.C., Miulescu, R.G., Petca, R.C., Petca, A., Dumitraşcu, M.C. & Şandru, F., *Teratogenic Effect of Isotretinoin in Both Fertile Females and Males*, Experimental and Therapeutic Medicine, **21**(5), pp. 1-5, 2021.
- [7] Widowati, W., Laksmiawati, D.R., Wargasetia, T.L., Afifah, E., Amalia, A., Arinta, Y. & Suciati, T., *Mangosteen Peel Extract (Garcinia mangostana L.) as Protective Agent in Glucose-induced Mesangial Cell as In Vitro Model of Diabetic Glomerulosclerosis*, Iranian Journal of Basic Medical Sciences, **21**(9), pp. 972-977, 2018.
- [8] Janardhanan, S., Mahendra, J., Mahendra, L. & Devarajan, N., *Cytotoxic Effects of Mangosteen Pericarp Extracts on Oral Cancer and Cervical Cancer Cells*, Asian Pacific Journal of Cancer Prevention: APJCP, **21**(9), 2577, 2020.
- [9] Chen, R., Zhang, H., Liu, P., Wu, X. & Chen, B., *Gambogenic Acid Synergistically Potentiates Bortezomib-induced Apoptosis in Multiple Myeloma*, Journal of Cancer, **8**(5), 839, 2017.
- [10] Kurniadewi, F., Aqilah, A.S., Kartika, I.R., Nurjayadi, M., Hermawati, E. & Danova, A., *Garciniaxanthone E and 12b-Hydroxy-des-D-garcigerrin A from The Tree Bark Garcinia dulcis and Their Inhibitory Properties Against Receptor Tyrosine Kinases*, Jurnal Kimia Valensi, **10**(1), pp. 20-26, 2024.
- [11] Li, J., Nie, X., Panthakarn Rangsinth, Wu, X., Zheng, C., Cheng, Y., Shiu, P.H., Li, R., Lee, S.M., Fu, C., Zhang, J. & Leung, G.P., *Structure and Activity*

- Relationship Analysis of Xanthenes from Mangosteen: Identifying Garcinone E As A Potent Dual EGFR and VEGFR2 Inhibitor*, *Phytomedicine*, **122**, 155140, 2024.
- [12] Kurniadewi, F., Palah, L.M., Kartika, I.R., Nurjayadi, M., Hermawati, E. & Danova, A., *Isolation, Characterization, and Evaluation of Xanthone Derivatives from Garcinia mangostana Twigs as Tyrosine Kinase Inhibitors with Potential EGFR Selectivity*, *Advanced Journal of Chemistry, Section A*, **8**(6), pp. 1027-1042, 2025.
- [13] Jiang, N., Dai, Q., Su, X., Fu, J., Feng, X. & Peng, J., *Role of PI3K/AKT Pathway in Cancer: The Framework of Malignant Behavior*, *Molecular Biology Reports*, **47**(6), pp. 4587-4629, 2020.
- [14] Ostini, A. & Mourtada-Maarabouni, M., *Investigation into the Role of Long-Non-Coding RNA MIAT in Leukemia*, *Non-Coding RNA*, **9**(4), 47, 2023.
- [15] Corzo Prada, L., Uruña, C., Leal-García, E., Barreto, A., Ballesteros-Ramírez, R., Rodríguez-Pardo, V. & Fiorentino, S., *Doxorubicin Activity Is Modulated by Traditional Herbal Extracts in a 2D and 3D Multicellular Sphere Model of Leukemia*, *Pharmaceutics*, **15**(6), pp. 1690, 2023.
- [16] Ye, X., Wang, L., Yang, X., Yang, J., Zhou, J., Lan, C. & Zeng, J., *Integrated Chemical Characterization, Network Pharmacology, and Transcriptomics to Explore the Mechanism of Sesquiterpenoids Isolated from *Gynura divaricata* (L.) DC Against Chronic Myelogenous Leukemia*, *Pharmaceutics*, **15**(11), 1435, 2022.
- [17] Widowati, W., Prahastuti, S., Hidayat, M., Hasianna, S.T., Wahyudianingsih, R., Eltania, T.F. & Kusuma, H.S.W., *Detam 1 Black Soybean Against Cisplatin-Induced Acute Renal Failure in Rat Models via Antioxidant, Anti-Inflammatory, and Anti-Apoptotic Potential*, *Journal of Traditional and Complementary Medicine*, **12**(4), pp. 426-435, 2022.
- [18] Widowati, W., Darsono, L., Lucianus, J., Setiabudi, E., Obeng, S.S., Stefani, S. & Rizal, R., *Butterfly Pea Flower (*Clitoria ternatea* L.) Extract Displays Antidiabetic Effects Through Antioxidant Activity, Reduced Hepatic GSK-3 $\beta$ , and Pancreatic Glycogen in Diabetes Mellitus and Dyslipidemia Rats*, *Journal of King Saud University-Science*, **35**(4), 102579, 2023.
- [19] Priyandoko, D., Widowati, W., Kusuma, H.S.W., Afifah, E., Wijayanti, C.R., Rizal, R. & Utomo, D.H., *Inflammation-Inhibitory Activity of Green Tea, Soybean, and Guava Extracts During SARS-CoV-2 Infection Through TNF Protein in Cytokine Storm*, *Computational Biology and Chemistry*, **105**, pp. 107898, 2023.
- [20] Banerjee P, Kemmler E, Dunkel M. & Preissner R., *ProTox 3.0: A Webserver for the Prediction of Toxicity of Chemicals*, *Nucleic Acids Research*, **52**(W1), pp. W513-W520, 2024.
- [21] Lister, I.N.E., Ginting, C.N., Girsang, E., Nataya, E.D., Azizah, A.M. & Widowati, W., *Hepatoprotective Properties of Red Betel (*Piper crocatum* Ruiz and Pav) Leaf Extract Toward H<sub>2</sub>O<sub>2</sub>-Induced HepG2 Cells via Anti-Inflammatory, Antinecrotic, and Antioxidant Potency*, *Saudi Pharmaceutical Journal*, **28**(10), pp. 1182-1189, 2020.
- [22] Widowati, W., Murti, H., Widyastuti, H., Laksmitawati, D.R., Rizal, R., Kusuma, H.S.W. & Bachtiar, I., *Decreased Inhibition of Proliferation and*

- Induction of Apoptosis in Breast Cancer Cell Lines (T47D and MCF7) Following Treatment with Conditioned Medium Derived from Hypoxia-Treated Wharton's Jelly MSCs Compared with Normoxia-Treated MSCs*, International Journal of Hematology-Oncology and Stem Cell Research, **15**(2), 77, 2021.
- [23] Abdullah, M.Z., Bakar, L.M., Othman, N., Taher, M., Rasad, M.S.B.A., Foong, F.H.N. & Ichwan, S.J.A., *Anti-cancer Activities of  $\beta$ -Mangostin Against Oral Squamous Cell Carcinoma*, Journal of International Dental and Medical Research, **15**(1), pp. 81-87, 2022.
- [24] Nauman, M.C. & Johnson, J.J., *The Purple Mangosteen (Garcinia mangostana): Defining The Anticancer Potential of Selected Xanthones*, Pharmacological Research, **175**, 106032, 2022.
- [25] Amjad, M.T., Chidharla, A. & Kasi, A., *Cancer Chemotherapy*, StatPearls Publishing, Treasure Island (FL), 2024.
- [26] Zhang, C., Yu, G. & Shen, Y., *The Naturally Occurring Xanthone  $\alpha$ -Mangostin Induces ROS-Mediated Cytotoxicity in Non-Small Cell Lung Cancer Cells*, Saudi Journal of Biological Sciences, **25**(6), pp. 1090-1095, 2018.
- [27] Li, K., Wu, L., Chen, Y., Li, Y., Wang, Q., Li, M. & Wang, Z., *Cytotoxic and Antiproliferative Effects of  $\beta$ -Mangostin on Rat C6 Glioma Cells Depend on Oxidative Stress Induction via PI3K/AKT/mTOR Pathway Inhibition*, Drug Design, Development and Therapy, pp. 5315-5324, 2020.
- [28] Kim, M., Chin, Y.W. & Lee, E.J.,  *$\alpha$ ,  $\gamma$ -Mangostins Induce Autophagy and Show Synergistic Effects with Gemcitabine in Pancreatic Cancer Cell Lines*, Biomolecules & Therapeutics, **25**(6), 609, 2017.
- [29] López-García, J., Lehocný, M., Humpolíček, P. & Sába, P., *HaCaT Keratinocytes Response on Antimicrobial Atelocollagen Substrates: Extent of Cytotoxicity, Cell Viability, and Proliferation*, Journal of Functional Biomaterials, **5**(2), pp. 43-57, 2014.
- [30] Kalick, L. S., Khan, H. A., Maung, E., Baez, Y., Atkinson, A. N., Wallace, C. E. & Bishayee, A., *Mangosteen for Malignancy Prevention and Intervention: Current Evidence, Molecular Mechanisms, and Future Perspectives*, Pharmacological Research, **188**, 106630, 2023.
- [31] Diab, K.A., Shafik, R.E. & Yasuda, S., *In Vitro Antioxidant and Antiproliferative Activities of Novel Orange Peel Extract and Its Fractions on Leukemia HL-60 Cells*, Asian Pacific Journal of Cancer Prevention, **16**(16), pp 7053-7060, 2015.
- [32] Zhamanbayeva, G.T., Aralbayeva, A.N., Murzakhmetova, M.K., Tuleukhanov, S.T. & Danilenko, M., *Cooperative Antiproliferative and Differentiation-Enhancing Activity of Medicinal Plant Extracts in Acute Myeloid Leukemia Cells*, Biomedicine & Pharmacotherapy, **82**, pp. 80-89, 2016.
- [33] Yuvanatemiya, V., Srean, P., Klangbud, W. K., Venkatachalam, K., Wongsu, J., Parametthanuwat, T. & Charoenphun, N., *A Review of the Influence of Various Extraction Techniques and the Biological Effects of Xanthones from Mangosteen (Garcinia mangostana L.) Pericarps*, Molecules, **27**(24), 8775, 2022.
- [34] Subarnbhesaj, A., Miyauchi, M., Chanbora, C., Mikuriya, A., Nguyen, P. T., Furusho, H. & Takata, T., *Roles of VEGF-Flt-1 Signaling in Malignant Behaviors of Oral Squamous Cell Carcinoma*, PLoS One, **12**(11), 0187092, 2017.

- [35] Wang, F., Yamauchi, M., Muramatsu, M., Osawa, T., Tsuchida, R. & Shibuya, M., *RACK1 Regulates VEGF/Flt1-Mediated Cell Migration via Activation of the PI3K/Akt Pathway*, *Journal of Biological Chemistry*, **286**(11), pp. 9097-9106, 2011.
- [36] Meng, X.Y., Zhang, H.X., Mezei, M. & Cui, M., *Molecular Docking: A Powerful Approach for Structure-Based Drug Discovery*, *Current Computer-Aided Drug Design*, **7**(2), pp. 146-157, 2011.
- [37] Das, D.R., Kumar, D., Kumar, P. & Dash, B.P., *Molecular Docking and Its Application in the Search for Antisickling Agents from *Carica papaya**, *Journal of Applied Biology and Biotechnology*, **8**(01), pp. 105-116, 2020.
- [38] Varshan, I. & Sankar, S., *Molecular Docking Analysis of Hydroxycyclavicol and Eugenol from Betel Leaves Against the Outer Membrane Protein (OmpH) of *Dialister pneumosintes*: ADMET Properties*, *Cureus*, **16**(2), pp. 1-8, 2024.
- [39] Fatimawali, Tallei, T.E., Kepel, B.J., Bodhi, W., Manampiring, A.E. & Nainu, F., *Molecular Insight into the Pharmacological Potential of *Clerodendrum minahassae* Leaf Extract for Type-2 Diabetes Management Using a Network Pharmacology Approach*, *Medicina*, **59**(11), 1899, 2023.
- [40] Dong, C., Zhang, N.J. & Zhang, L.J., *Oxidative Stress in Leukemia and Antioxidant Treatment*, *Chinese Medical Journal*, **134**(16), pp. 1897-1907, 2021.
- [41] Fadil Amrulloh, L.S.W., Harmastuti, N., Prasetyo, A. & Herowati, R., *Analysis of Molecular Docking and Dynamics Simulation of Mahogany (*Swietenia macrophylla* King) Compounds Against the PLpro Enzyme SARS-COV-2*, *Pharmacy & Pharmaceutical Sciences Journal*, **10**(3), pp. 347-359, 2023.
- [42] Seo, S., Choi, J., Park, S. & Ahn, J., *Binding Affinity Prediction for Protein-Ligand Complexes Using a Deep Attention Mechanism Based on Intermolecular Interactions*, *BMC Bioinformatics*, **22**(1), pp. 1-15, 2021.
- [43] Tallei, T.E., Tumilaar, S.G., Niode, N.J., Fatimawali, F., Kepel, B.J., Idroes, R. & Emran, T.B., *Potential of Plant Bioactive Compounds as SARS-CoV-2 Main Protease (Mpro) and Spike (S) Glycoprotein Inhibitors: A Molecular Docking Study*, *Scientifica*, **2020**(1), 6307457, 2020.
- [44] Ferenczy, G.G. & Kellermayer, M., *Contribution of Hydrophobic Interactions to Protein Mechanical Stability*, *Computational and Structural Biotechnology Journal*, **20**, pp. 1946-1956, 2022.
- [45] Lipinski, C.A., Lombardo, F., Dominy, B.W. & Feeney, P.J., *Experimental and Computational Approaches to Estimate Solubility and Permeability in Drug Discovery and Development Settings*, *Advanced Drug Delivery Reviews*, **23**(1-3), pp. 3-25, 1997.
- [46] Asano, D., Takakusa, H. & Nakai, D., *Oral Absorption of Middle-to-Large Molecules and Its Improvement, with A Focus on New Modality Drugs*, *Pharmaceutics*, **16**(1), 47, 2023.
- [47] Doak, B.C., Zheng, J., Dobritzsch, D. & Kihlberg, J., *How Beyond Rule of 5 Drugs and Clinical Candidates Bind to Their Targets*, *Journal of Medicinal Chemistry*, **59**(6), pp. 2312-2327, 2015.
- [48] Kenny, P.W., *Hydrogen Bond Donors in Drug Design*, *Journal of Medicinal Chemistry*, **65**(21), pp. 14261-14275, 2022.